

Detecting Adversarial Data via Perturbation Forgery

Qian Wang¹, Chen Li², Yuchen Luo², Hefei Ling^{1*}, Ping Li¹, Jiazhong Chen¹, Shijuan Huang¹,
Ning Yu³

¹Huazhong University of Science and Technology, China

²Wuhan University, China

³Netflix Eyeline, USA

{yqwq1996,lhefei,lpshome,jzchen,shijuan_huang}@hust.edu.cn, {lichenc, yuchenluo}@whu.edu.cn,
ningyu.hust@gmail.com

Abstract

As a defense strategy against adversarial attacks, adversarial detection aims to identify and filter out adversarial data from the data flow based on discrepancies in distribution and noise patterns between natural and adversarial data. Although previous detection methods achieve high performance in detecting gradient-based adversarial attacks, new attacks based on generative models with imbalanced and anisotropic noise patterns evade detection. Even worse, existing techniques either necessitate access to attack data before deploying a defense or incur a significant time cost for inference, rendering them impractical for defending against newly emerging attacks that are unseen by defenders. In this paper, we explore the proximity relationship between adversarial noise distributions and demonstrate the existence of an open covering for them. By learning to distinguish this open covering from the distribution of natural data, we can develop a detector with strong generalization capabilities against all types of adversarial attacks. Based on this insight, we heuristically propose Perturbation Forgery, which includes noise distribution perturbation, sparse mask generation, and pseudo-adversarial data production, to train an adversarial detector capable of detecting unseen gradient-based, generative-based, and physical adversarial attacks, while remaining agnostic to any specific models. Comprehensive experiments conducted on multiple general and facial datasets, with a wide spectrum of attacks, validate the strong generalization of our method.

Introduction

Numerous studies have demonstrated the effectiveness of deep neural networks (DNNs) in various tasks (Shi et al. 2020). However, it is also well-known that DNNs are vulnerable to adversarial attacks, which generate adversarial data by adding imperceptible perturbations to natural images, potentially causing the model to make abnormal predictions. This vulnerability reduces the reliability of deep learning systems, highlighting the urgent need for defense techniques. Some approaches employ adversarial training techniques (Zhang et al. 2019), which incorporate adversarial data into the training process to inherently bolster the model’s immunity against adversarial noise (adv-noise). Other methods utilize adversarial purification (Yoon, Hwang, and Lee 2021) to cleanse the input data of adv-noise

before model inference. Unfortunately, adversarial training often results in diminished classification accuracy on adversarial data and may sacrifice performance on natural data. While purification techniques may seem more reliable, the denoising process can inadvertently smooth the high-frequency texture of clean images, leading to suboptimal accuracy on both natural and adversarial images.

Another branch of adversarial defense is adversarial detection (Feinman et al. 2017; Ma et al. 2018), which aims to filter out adversarial data before they are fed into target systems. These methods rely on discerning the discrepancies between adversarial and natural distributions, thereby maintaining the integrity of target systems while achieving high performance in defending against adversarial attacks. However, existing adversarial detection approaches primarily train specialized detectors tailored for specific attacks or classifiers (Deng et al. 2021), which may not generalize well to unseen advanced attacks.

Some recent approaches (Zhang et al. 2023; Wang et al. 2023a) have attempted to enhance the generalization of adversarial detectors by leveraging diffusion models and manually designed pseudo-noise. Nevertheless, as shown in Table 1, this improvement often comes at the cost of increased inference time, and even well-trained detectors still struggle with adversarial data produced by generative models such as generative adversarial networks (GANs) and diffusion models. Specifically, generative-based adversarial attacks, such as M3D (Zhao et al. 2023) and Diff-PGD (Xue et al. 2024), are recently developed techniques designed to generate more natural adversarial data. Unlike traditional gradient-based attacks like PGD (Madry et al. 2017), generative-based attacks tend to create imbalanced and anisotropic perturbations that are intense in high-frequency and salient areas but mild in low-frequency and background areas. These perturbations circumvent all current adversarial detection methods, posing a new challenge to the field. Therefore, there is an urgent need for a low-time-cost detection method with strong generalization performance against both unseen gradient-based attacks and unseen generative-based attacks.

In this paper, we investigate the association between the distributions of different adv-noises. As shown in Figure 1, by modeling noise as multivariate Gaussian distributions, we define the proximity relationship of the noise distributions in a metric space and establish a perturbation method

*Corresponding author

Table 1: **Properties of our method vs Other Adversarial Detection:** We summarize four metrics for adversarial detection. “Detect Attacks” means what kind of attacks the method is designed to detect. “Attack-Agnostic” describes whether the detection can detect unseen attack types. “Model-Agnostic” describes whether the method is independent of the protected model. Finally, “Time Cost” measures the time cost of a detector during inference.

Methods	Detect Attacks	Attack-Agnostic	Model-Agnostic	Time Cost
LID (Ma et al. 2018)	Gradient	×	×	*
LiBRe (Deng et al. 2021)	Gradient	✓	×	*
EPSAD (Zhang et al. 2023)	Gradient	✓	✓	**
SPAD (Wang et al. 2023a)	Gradient + GAN	✓	✓	*
Ours	Gradient + GAN + Diffusion	✓	✓	*

to construct the proximal distributions. Based on these assumptions and definitions, we demonstrate that all adv-noise distributions are proximal using the Wasserstein distance, and we deduce a corollary that an open covering of the adv-noise distributions exists. We then propose the core idea of this paper: **by learning to distinguish the open covering of adv-noise distributions from the natural distribution, we obtain a detector with strong generalization performance against all types of unseen attacks.**

Based on this idea, we propose Perturbation Forgery, a pseudo-adversarial data generation method designed to train a detector with strong generalization capabilities for detecting all types of adversarial attacks. As shown in Figure 2, Perturbation Forgery comprises noise distribution perturbation, sparse mask generation, and pseudo-adversarial data (pseudo-adv-data) production. By continuously perturbing the noise distribution of a commonly used attack, such as FGSM (Goodfellow, Shlens, and Szegedy 2014), we obtain a nearly complete family of distributions that form the aforementioned open covering. Simultaneously, sparse masks are generated using attention maps and saliency maps of the natural data, converting the sampled global noises into local forms to help the detector focus on local noise patterns so as to detect generative-based adv-noise. Sampling noises from the perturbed noise distributions, we sparsify these noises with the sparse masks and inject them into natural data. This process converts half of the natural data into pseudo-adv-data, which are then combined with the remaining uncontaminated data to train the binary adversarial detector. To the best of our knowledge, we are the first to empower a detector with the robust ability to detect all types of adversarial attacks, including gradient-based, GAN-based, diffusion-based, and physical attacks, with minor time cost.

Our contributions are summarized in four thrusts:

- By modeling adversarial noise as Gaussian distributions, we investigate the association between different adversarial noise distributions and demonstrate their proximity in a metric space.
- Based on our assumptions and definitions, we deduce the existence of an open covering for adv-noise distributions and propose training a detector to distinguish this open covering from the natural data distribution, thereby achieving strong generalization.
- Building on our deductions, we propose Perturbation Forgery, which includes noise distribution perturbation,

sparse mask generation, and pseudo-adversarial data production. This method is designed to train a binary detector with strong generalization performance against all types of unseen attacks, including gradient-based, GAN-based, diffusion-based, and physical adversarial data, with minor time cost.

- We conduct evaluations on multiple general and facial datasets across a wide spectrum of gradient-based, generative-based, and physical attacks, demonstrating the consistently strong performance of our method in adversarial detection tasks.

Related Work

Adversarial Attack

Gradient-based adversarial attack Adversarial attacks (Goodfellow, Shlens, and Szegedy 2014; Madry et al. 2017; Kurakin, Goodfellow, and Bengio 2016) attempt to fool a classifier into changing prediction results by injecting subtle perturbations to the input data while maintaining imperceptibility from human eyes. In an effort to improve transferability under the black-box setting, DIM (Wu et al. 2021), SIM (Lin et al. 2019), and VIM (Wang and He 2021) are recent attacks and achieve a high attack rate against several defense techniques.

Generative-based Adversarial Attacks Recently, another branch of attack uses generative models to make adversarial data with a more natural style and imbalanced noise compared to gradient-based attacks. Among them, CDA (Naseer et al. 2019), TTP (Naseer et al. 2021), and M3D (Zhao et al. 2023) utilize GAN to craft adversarial data and achieve higher efficiency when attacking large-scale datasets. Diff-Attack (Chen et al. 2023) and Diff-PGD (Xue et al. 2024) employ the diffusion model as a strong prior to better ensure the realism of generated data. Designed for perturbing facial recognition systems, AdvMakeup (Yin et al. 2021) and AMT-GAN (Hu et al. 2022) are presented to generate imperceptible adversarial images of the face.

In this paper, a wide spectrum of gradient-based generative-based and adversarial attacks on ImageNet and facial datasets is used to for evaluation.

Adversarial Detection

As one of the technical solutions to ensure the safety of DNNs, there has been a significant amount of exploration

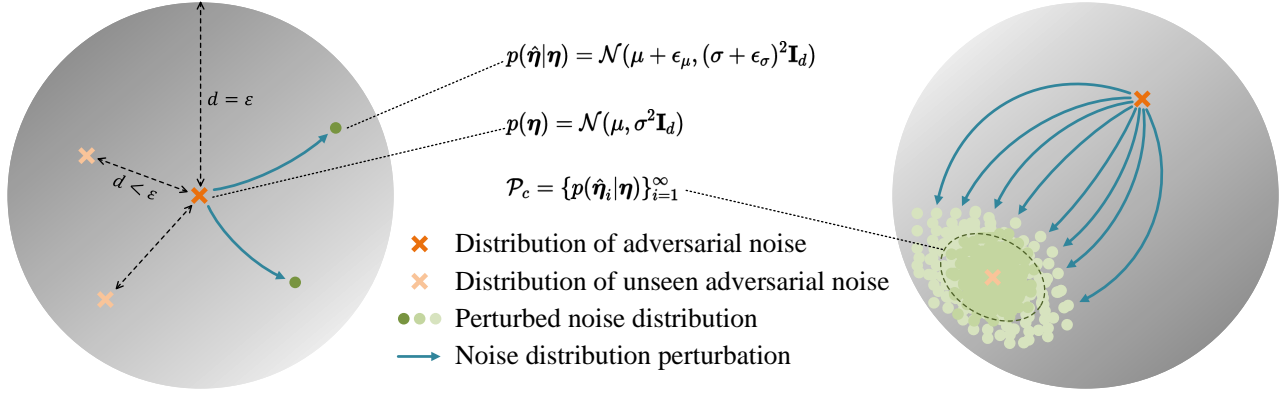


Figure 1: Illustration of the proximity of adv-noise distributions and perturbed noise distributions. Left: all the distributions of adv-noise and the perturbed distributions are in a ϵ -ball centered on a given adv-noise distribution. Right: by continuously perturbing the commonly used adv-noise distribution, we obtain an open covering of distributions of adversarial noise.

in the field of adversarial detection (Ma et al. 2018). Li-BrE (Deng et al. 2021) leverages Bayesian neural networks to endow pre-trained DNNs with the ability to defend against unseen adversarial attacks, SPAD (Wang et al. 2023a) leverages a data augmentation method to detect adversarial face images from unseen attack, while EP-SAD (Zhang et al. 2023) incorporates a diffusion model to detect adversarial data with minimal perturbation magnitude, albeit at the cost of inference time.

While current methods have achieved remarkable improvements in adversarial detection, generative-based adversarial attacks can easily circumvent them, posing a new challenge. To address the problems above, our method is proposed to detect all types of unseen attacks, including gradient-based, generative-based, and physical attacks.

Proximity of Adversarial Noise Distribution

In this section, we provide an overview of preliminary concepts related to adversarial data generation and explore the relationship between adversarial noise distributions. We define the proximity of noise distributions and examine the imperceptibility of adversarial noise. Following this, we present the core idea of this paper: by learning to distinguish the open covering of adversarial noise distributions from the natural distribution, we develop a detector with strong generalization capabilities against all types of unseen attacks.

Adversarial data generation Given a DNN f that works on dataset $\mathcal{D} = \{(\mathbf{x}_i, y_i)\}_{i=1}^n$ with $(\mathbf{x}_i \in \mathcal{X}, y_i \in \mathcal{C})$ being (sample, ground-truth) pair, an adversarial example $\hat{\mathbf{x}}$ regarding sample \mathbf{x} with perturbation magnitude ϵ is calculated as:

$$\hat{\mathbf{x}} = \underset{\hat{\mathbf{x}} \in \mathcal{B}(\mathbf{x}, \epsilon)}{\operatorname{argmax}} \mathcal{L}(f(\hat{\mathbf{x}}), y), \quad (1)$$

where \mathcal{L} is some loss function and $\mathcal{B}(\mathbf{x}, \epsilon) = \{\mathbf{x}' | \ell^p(\mathbf{x}, \mathbf{x}') < \epsilon\}$ restricts the perturbation under ℓ^p norm. Following (Goodfellow, Shlens, and Szegedy 2014), we simply denote adversarial sample as $\hat{\mathbf{x}} = \mathbf{x} + \eta$.

Proximity of noise distribution Due to the subtle and imperceptible nature of adv-noise, adversarial data and natural

data appear visually similar. Thus, we assume that this similarity also exists between the noises of different adversarial attacks. To investigate the similarity of these noises, we provide the following definition, which depicts a close relationship between two independent noise distributions:

Definition 1 (Proximal Noise Distribution). Let P and Q be the distribution functions of two independent noise samples \mathbf{x}_1 and \mathbf{x}_2 . We call them proximal noise distributions under ϵ if we have a metric $d(\cdot, \cdot)$ and $\exists \epsilon > 0$, s.t.

$$d(P, Q) < \epsilon. \quad (2)$$

A common assumption for instance feature distribution is to model it as a Gaussian distribution (Du et al. 2022). Obtained by subtracting from clean data and adversarial data, adv-noises naturally form a Gaussian distribution. Therefore, we assume that noise r.v η satisfied truncated Gaussian distribution $\mathcal{N}(\mu, \sigma^2 \mathbf{I}_d)$ with its truncated interval is $[-\epsilon, \epsilon]^d$. Built upon Definition 1, we derive the following theorem about the association between the distributions of different adv-noises:

Theorem 1. Let \mathcal{P}_a be the distribution set composed of all the adversarial noise distributions. Given independent noise distributions $Q_i, i \in N^+$. For $\forall i \neq j, Q_i$ and Q_j are proximal noise distributions if the following conditions are met.

- 1) if $Q_i, Q_j \in \mathcal{P}_a$.
- 2) if $\exists \epsilon_\mu, \epsilon_\sigma > 0$ s.t. $\|\mu_i - \mu_j\| < \epsilon_\mu$ and $|\sigma_i - \sigma_j| < \epsilon_\sigma$ where the $\|\cdot\|$ is a Euclidean norm on \mathbb{R}^n .

Theorem 1 tells us: 1) All adversarial noise distributions are proximal noise distributions. 2) If the parameters of two noise distributions are sufficiently close to those of a given distribution, we can regard these two distributions as proximal noise distributions.

We can further deduce several corollaries of the theorem. 1) All noise distributions proximal to the known adversarial distribution $p(\eta)$ form an open ϵ -ball centered on $p(\eta)$, denoting as $\mathcal{P}_\epsilon = \{p(\eta_i) | d(p(\eta_i), p(\eta)) < \epsilon\}$, and also form a metric space $(\mathcal{P}_\epsilon, d)$. 2) The adv-noise distribution set is also located in this ball: $\mathcal{P}_a \subset \mathcal{P}_\epsilon$. 3) Based on the properties of the metric space $(\mathcal{P}_\epsilon, d)$, for all subset $\mathcal{P}_i \subset \mathcal{P}_\epsilon$, there exists an open covering of the subset: $\mathcal{P}_i \subset \{G_c\}_{c \in J}$.

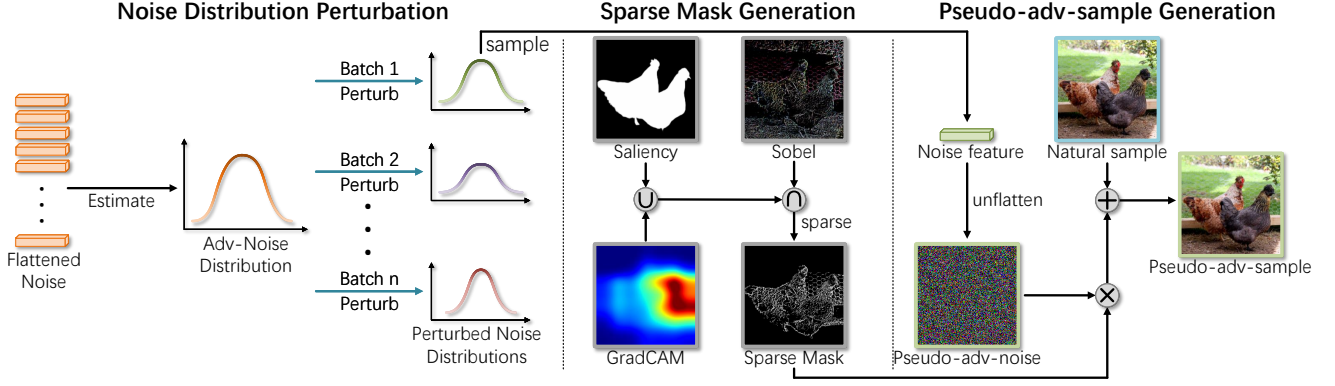


Figure 2: Illustration of Perturbation Forgery. Before training, we estimate the noise distribution of a commonly used attack and continuously perturb it in each batch. After that, we sample noises from the perturbed distribution and convert them into local noise using sparse masks. Finally, pseudo-adversarial data is generated by adding these local noises to the natural samples.

Based on the corollaries, we deduce the core idea of this paper: Let $p(\hat{\eta}_i|\eta) = \mathcal{N}(\mu + \epsilon_{\mu i}, (\sigma + \epsilon_{\sigma i})^2 \mathbf{I}_d)$, $i = 1, 2, \dots, n$ denote generated proximal noise distributions of the given adv-noise distribution $p(\eta) = \mathcal{N}(\mu, \sigma^2 \mathbf{I}_d)$ where $\epsilon_{\mu i}, \epsilon_{\sigma i}$ are randomly sampled from uniform distributions and restricted by $\epsilon_{\mu i}, \epsilon_{\sigma i} < \epsilon$. As shown in Figure 1, **when $n \rightarrow \infty$, we can always obtain a distribution set $\mathcal{P}_c = \{p(\hat{\eta}_i|\eta)\}_{i=1}^{\infty}$ that forms an open covering of the adversarial distribution set \mathcal{P}_a . Trained with the open covering, the detector can distinguish the distributions of natural data and adversarial data, thereby having the functionality to detect unseen adversarial attacks.**

For proofs of theorem and corollaries, please refer to the supplementary materials.

Perturbation Forgery

Based on the theory support in the last section, we heuristically propose Perturbation Forgery to train a detector with strong generalization against all types of unseen attacks.

As illustrated in Figure 2, Perturbation Forgery encompasses three elements: distribution perturbation, sparse mask generation, and pseudo-adversarial data production. At first, the noise distribution of a commonly used attack is continuously perturbed using **Noise Distribution Perturbation** into numerous noise distributions that remain proximal to the original, thereby forming the open covering. After that, we sample noises from the perturbed distribution and convert them into sparse local noise using **Sparse Mask Generation**. Subsequently, we convert half of the natural data into pseudo-adversarial data using **Pseudo-Adversarial Data Generation** and train a binary detector on the these data along with the remaining natural data.

Noise Distribution Perturbation

Given the training dataset $\{(\mathbf{x}_k, y_k)\}_{k=1}^n$ composed by natural data, we add adv-noise on it using a commonly used attack (such as FGSM) and generate adversarial noise features $\mathcal{D}_{\text{noise}} := \{\mathbf{z}_k = h(\eta_k)\}_{k=1}^n$ by

$$\eta_k = \text{Attack}(\mathbf{x}) - \mathbf{x}, k \in [1, n], \quad (3)$$

where $h : \mathcal{X} \rightarrow \mathbb{R}^d$ is the flattening operation that converts multidimensional data into vectors.

Assuming the noise features form a multivariate Gaussian distribution $p(\mathbf{z}) = \mathcal{N}(\boldsymbol{\mu}, \boldsymbol{\Sigma})$ (Du et al. 2022), we estimate the parameters mean $\boldsymbol{\mu}$ and covariance $\boldsymbol{\Sigma}$ of $\mathcal{D}_{\text{noise}}$ by

$$\hat{\boldsymbol{\mu}} = \frac{1}{N} \sum_k \mathbf{z}_k, \quad \hat{\boldsymbol{\Sigma}} = \frac{1}{N} \sum_k (\mathbf{z}_k - \hat{\boldsymbol{\mu}})(\mathbf{z}_k - \hat{\boldsymbol{\mu}})^\top. \quad (4)$$

For the i^{th} batch of training, we perturb the estimated distribution to a proximal noise distribution by

$$\hat{\boldsymbol{\mu}}_i = \hat{\boldsymbol{\mu}} + \alpha_i \cdot \mathbf{m}_i, \quad \hat{\boldsymbol{\Sigma}}_i = \hat{\boldsymbol{\Sigma}} + \beta_i \cdot \mathbf{V}_i, \quad (5)$$

where $\mathbf{m}_i \sim \mathcal{N}(0, \mathbf{I}_d)$ and $\mathbf{V}_i \sim \mathcal{N}(0, \mathbf{I}_{d \times d})$ are vector and matrix of perturbation. $\alpha_i \sim \mathcal{U}(-\epsilon_\mu, \epsilon_\mu)$ and $\beta_i \sim \mathcal{U}(0, \epsilon_\sigma)$ are scale parameters sampled from uniform distributions. After n batches of training, we have a perturbed distribution set $\{\mathcal{N}(\hat{\boldsymbol{\mu}}_i, \hat{\boldsymbol{\Sigma}}_i)\}$, thereby forming the approximate open covering \mathcal{P}_c . Trained with \mathcal{P}_c , the detector can distinguish the distributions of natural and adversarial data.

Sparse Mask Generation

Unlike gradient-based adversarial attacks, generative-based attacks tend to generate imbalanced and anisotropy perturbations, showing much intensity in high-frequency and salient areas and mild in low-frequency and background areas. Besides, in the physical situation, adversarial attacks also tend to add patches to local areas. Noticing this, we propose sparse masks to perturbation forgery to assist the detector in detecting local adv-noises.

Previous research has demonstrated that the spectra of real and fake images differ significantly in high-frequency regions (Luo et al. 2021). Additionally, generative-based adversarial data manipulate characteristics, such as abnormal color aberrations, in these high-frequency regions (Wang et al. 2023a). To augment the detection performance on generative-based adversarial data, we need to sparse the pseudo-noise sampled from perturbed noise distribution and highlight the noise in high-frequency regions to mimic the style of generative-based attacks.

Algorithm 1: Training Procedure with Perturbation Forgery

Input: Training dataset, initial attack Attack, saliency detection model f_s , and GradCAM model f_c .

Output: A detector with strong generalization capabilities against all types of unseen attacks.

- 1: Generate adversarial noise using the initial attack Attack in Eq. 3.
 - 2: Estimate a multivariate Gaussian distribution $p(\mathbf{z}) = \mathcal{N}(\hat{\boldsymbol{\mu}}, \hat{\boldsymbol{\Sigma}})$ of adv-noise using Eq. 4.
 - 3: **for** batch i **in** $1, \dots, n$ **do**
 - 4: Generate a perturbed noise distribution $p(\mathbf{z}_i) = \mathcal{N}(\hat{\boldsymbol{\mu}}_i, \hat{\boldsymbol{\Sigma}}_i)$ using Eq. 5.
 - 5: **for** sample $\mathbf{x}_{i,k}$ half of batch i **do**
 - 6: Generate sparse masks $\text{Mask}(\mathbf{x}_{i,k})$ using Eq. 8.
 - 7: Sample pseudo-adversarial noise $\hat{\boldsymbol{\eta}}_{i,k}$ using Eq. 10.
 - 8: Generate pseudo-adversarial data $\hat{\mathbf{x}}_{i,k}$ using Eq. 12.
 - 9: **end for**
 - 10: Train the detector on batch i .
 - 11: **end for**
-

Given this, we first mask the high-frequency area of a natural sample using saliency detection (Qin et al. 2019) and GradCAM (Selvaraju et al. 2017):

$$\text{Mask}_1(\mathbf{x}) = \text{Map}(f_s(\mathbf{x}); \gamma_s) \cup \text{Map}(f_c(\mathbf{x}); \gamma_c), \quad (6)$$

where f_s and f_c are the saliency detection model and GradCAM model respectively. $\text{Map}(\mathbf{x}; \gamma)$ is a binary indicator function parameterized by γ :

$$\text{Map}(\mathbf{x}; \gamma) = \text{Clip}_{[0,1]}(\mathbf{x} - \gamma \mathbf{I}_{\mathcal{X}}). \quad (7)$$

The noise that occurs in the high-frequency region tends to occupy only a small part of the region rather than spreading to the entire high-frequency spectrum. Therefore, we select the high-frequency point using the Sobel operator (Duda and Hart 1973) to sparsify the mask of sample $\mathbf{x}_{i,k}$:

$$\text{Mask}_2(\mathbf{x}) = \text{Map}(\text{Sobel}(\mathbf{x}); \gamma_l), \quad (8)$$

$$\text{Mask}(\mathbf{x}_{i,k}) = \text{Mask}_1(\mathbf{x}_{i,k}) \cap \text{Mask}_2(\mathbf{x}_{i,k}). \quad (9)$$

Pseudo-Adversarial Data Production

For the i^{th} batch of training, we sample pseudo-adversarial noise from the perturbed distribution by:

$$\hat{\boldsymbol{\eta}}_{i,k} = h^{-1}(\mathbf{z}_{i,k}), \quad (10)$$

$$\mathbf{z}_{i,k} \in \{\mathbf{z}_k | \mathbf{z}_k \sim \mathcal{N}(\hat{\boldsymbol{\mu}}_i, \hat{\boldsymbol{\Sigma}}_i) \text{ and } p(\mathbf{z}_k) < \gamma_p\} \quad (11)$$

where $h^{-1} : \mathbb{R}^d \rightarrow \mathcal{X}$ is an inverse function of h to unflatten noise features, and γ_p is a threshold that excludes data with a low likelihood. Note that $\boldsymbol{\eta}_i$ is a global noise and needs to be localized by a sparse mask. For natural data $\mathbf{x}_{i,k}$ in the i^{th} batch, the corresponding pseudo-adversarial data $\hat{\mathbf{x}}_{i,k}$ is produced by adding the masked local noise to it:

$$\hat{\mathbf{x}}_{i,k} = \mathbf{x}_{i,k} + \hat{\boldsymbol{\eta}}_{i,k} \otimes \text{Mask}(\mathbf{x}_{i,k}). \quad (12)$$

where \otimes is Hadamard product.

For each batch, we convert half of the natural data to pseudo-adversarial data by Perturbation Forgery and train a binary detector using the Cross-Entropy classification loss (Zhang and Sabuncu 2018). The overall training procedure with Perturbation Forgery is presented in Algorithm 1.

Experiments

To validate the detection performance of our approach against various adversarial attack methods, we conduct extensive experiments on multiple general and facial datasets.

Experiment Settings

Datasets and Network Architectures The datasets for evaluation include 1) general dataset ImageNet100 (Deng et al. 2009), and 2) face datasets: Makeup (Gu et al. 2019), CelebA-HQ (Karras et al. 2017), and LFW (Gary et al. 2007). Gradient-based attacks and generative-based attacks are launched only on ImageNet100. For face attacks, we conduct Adv-Makeup on Makeup, AMT-GAN on CelebA-HQ, and physical attacks on LFW.

Adversarial Attacks We adopt 9 gradient-based attacks, 5 generative-based attacks, and 6 face attacks to evaluate our method. For gradient-based attacks, BIM (Kurakin, Goodfellow, and Bengio 2016), PGD (Madry et al. 2017), RFGSM (Tramèr et al. 2018), MIM (Dong et al. 2018), DIM (Wu et al. 2021), NIM and SNIM (Lin et al. 2019), VNIM (Wang and He 2021), and Auto-Attack (Croce and Hein 2020) are used as the unseen attacks. For generative-based attacks, we adopt 3 GAN-based attacks including CDA (Naseer et al. 2019), TTP (Naseer et al. 2021), and M3D (Zhao et al. 2023), and 2 Diffusion-based attacks including Diff-Attack (Chen et al. 2023) and Diff-PGD (Xue et al. 2024) to craft adv-samples. For face attacks, 1 gradient-based attack TIPIM (Yang et al. 2021), 2 GAN-based attacks including AdvMakeup (Yin et al. 2021) and AMT-GAN (Hu et al. 2022), and 3 physical attacks including Adv-Sticker (Tong et al. 2021), Adv-Glasses (Sharif et al. 2016), and Adv-Mask (Tong et al. 2021) produce adversarial face samples. For each of the above attack methods, adversarial data is generated with the perturbation magnitude of $\epsilon = 4/255$ (except for the unrestricted attacks) following (Zhang et al. 2023).

Baselines We compare our method with state-of-the-art detection methods across three research fields, including adversarial detection, synthetic image detection, and face forgery detection, evaluating the detection of various types of adversarial attacks. For detecting gradient-based attacks, we compared our method with adversarial detection methods including LID (Ma et al. 2018), LiBre (Deng et al. 2021), SPAD (Wang et al. 2023a), and EPSAD (Zhang et al. 2023). Since existing adversarial detection methods do not address generative-based adversarial data, we compared our method with synthetic image detection methods including CNN-Detection(Wang et al. 2020), LGrad(Tan et al. 2023), Universal-Detector(Ojha, Li, and Lee 2023), and DIRE(Wang et al. 2023b) for detecting generative-based attacks. For detecting GAN-based face attacks, we compared with face forgery detection methods including Luo

Table 2: Comparison of AUC scores (%) of detecting gradient-based attacks on ImageNet100.

Detector	BIM	PGD	RFSGM	DIM	MIM	NIM	VNIM	SNIM	AA
LID (Ma et al. 2018)	0.9782	0.9750	0.9637	0.8942	0.9146	0.8977	0.8865	0.8752	0.9124
LiBRe (Deng et al. 2021)	0.9259	0.9548	0.9769	0.9243	0.8725	0.9013	0.8862	0.8694	0.8653
SPAD (Wang et al. 2023a)	0.9846	0.9851	0.9833	0.9815	0.9820	0.9823	0.9891	0.9877	0.9890
EPSAD (Zhang et al. 2023)	0.9998	0.9989	0.9992	0.9923	0.9918	0.9972	0.9946	0.9908	0.9998
ours	0.9911	0.9912	0.9911	0.9863	0.9931	0.9934	0.9878	0.9914	0.9941

Table 3: Comparison of AUC scores of detecting generative-based attacks on ImageNet100.

Detector	CDA	TTP	M3D	Diff-Attack	Diff-PGD
CNN-Detection (Wang et al. 2020)	0.7051	0.6743	0.6917	0.3963	0.526
LGrad (Tan et al. 2023)	0.6144	0.6077	0.6068	0.5586	0.5835
Universal-Detector (Ojha, Li, and Lee 2023)	0.7945	0.8170	0.8312	0.9202	0.5531
DIRE (Wang et al. 2023b)	0.8976	0.9097	0.9129	0.9097	0.9143
EPSAD	0.9674	0.6997	0.7265	0.4700	0.1507
SPAD	0.9385	0.9064	0.8984	0.8862	0.8879
ours	0.9878	0.9678	0.9364	0.9223	0.9223

et al. (Luo et al. 2021), He et al. (He et al. 2021), and ODIN (Liang, Li, and Srikant 2017). We conducted experiments using the pre-trained models and authors’ implementation code of the above methods.

Evaluation Metrics Following previous adversarial detection works (Zhang et al. 2023), we employ the Area Under the Receiver Operating Characteristic Curve (AUC) as the primary evaluation metric to assess the performance of our classification models. The AUC is a widely recognized metric in the field of machine learning and is particularly useful for evaluating binary classification problems. For fair comparisons, the number of natural data and adversarial data in the experiments remained consistent.

Implementation details XceptionNet (Chollet 2017) is selected as our backbone model and is trained on all the above datasets. For adv-noise distribution estimation, we utilize Torchattacks (Kim 2020) to generate 1000 noise images for each dataset. The uniform distribution parameters are set as $\epsilon_\mu = 3$ and $\epsilon_\sigma = 0.005$. The threshold of the sample control is set as $\gamma_s = 0.05$. The thresholds of the binary indicator function are set as $\gamma_s = 0$, $\gamma_c = 125$ and $\gamma_l = 100$. FGSM (Goodfellow, Shlens, and Szegedy 2014) is used as the initial attack for Perturbation Forgery. Training epochs are set to 10 and convergence is witnessed.

Detecting Gradient-based Attacks

We begin by comparing our method with state-of-the-art techniques in detecting gradient-based attacks on ImageNet100. All the attacks are seen to LID but unseen to other baselines and our method. For each attack, 1,000 adversarial images are generated in the white-box setting to test the detection models. All baseline methods are sourced from existing adversarial detection research. As reported in Table 2, although EPSAD performs well, our method demonstrates effective detection (achieving an AUC score of 0.9931 against MIM and 0.9914 against SNIM) across a variety of attack methods. These results validate our assumptions about the proximity of the noise distribution. By continuously perturbing the estimated noise distribution of a given attack

(FGSM), we obtain an open covering noise of distributions from all the attacks. Given one seen attack, we are able to detect all the unseen attacks. The consistent detection performance verifies the effectiveness of our core idea of training a detector to distinguish the open covering of adv-noise distributions from natural ones and demonstrates the strong generalization capability of our method against gradient-based attacks. Additional results on CIFAR10 are provided in the supplementary materials.

Detecting generative-based Attacks

To investigate the advantage of our method in detecting generative-based attacks, we compare with state-of-the-art methods of synthetic image detection and adversarial detection methods on ImageNet100. As shown in Table 3, our method substantially surpasses other methods, exhibiting highly effective detection capabilities. For adversarial detection baselines, due to the noise produced by generative models tending to be imbalanced compared to perturbations of traditional gradient-based attacks, these methods struggle to conduct effective detection. In contrast, with the assistance of sparse masks, our detector can perceive the local noises brought by GAN and diffusion models. As adversarial data is crafted from natural data, most synthetic image detection methods lose their effectiveness except DIRE(Wang et al. 2023b). This is probably because DIRE leverages the reconstruction error of images generated by diffusion models, thus maintaining a certain level of effectiveness.

Detecting Face Adversarial Examples

Adversarial attack on the face recognition model is an important branch of adversarial example research. Therefore, the detection ability of adversarial face examples is an important indicator of the performance of the detector. We perform various adversarial face attacks and compare our approach with state-of-the-art methods from adversarial face detection and face forgery detection. As shown in Table 4, our method shows excellent performance against a variety of adversarial attacks targeting faces and surpasses many existing adversarial face detection techniques. It further indicates

Table 4: Comparison of AUC scores for detecting various adversarial attacks on the face.

Detector	TIPIM	Adv-Sticker	Adv-Glasses	Adv-Mask	Detector	Adv-Makeup	AMT-GAN
LID	0.6974	0.5103	0.6472	0.5319	He et al. (He et al. 2021)	0.5252	0.8823
LiBRe	0.5345	0.9739	0.8140	0.9993	Luo et al. (Luo et al. 2021)	0.6178	0.6511
EPSAD	0.9647	0.9462	0.9260	0.9578	ODIN(Liang, Li, and Srikant 2017)	0.6325	0.6970
SPAD	0.9256	0.9975	0.9244	0.9863	SPAD	0.9657	0.8969
ours	0.9885	0.9999	0.9999	0.9999	ours	0.9762	0.9216

Table 5: Ablation study on masks.

Ablation	CDA	TTP	M3D	Diff-Attack	Diff-PGD
w/o f_s	0.9755	0.9585	0.9320	0.9197	0.9135
w/o f_c	0.9864	0.9510	0.9262	0.9031	0.9062
w/o Sobel	0.9868	0.7235	0.6984	0.5231	0.5547

Table 6: Time cost of inference (second) on ImageNet100

Detector	LID	LiBRe	EPSAD	SPAD	ours
Time (second)	1.80	2.56	396.81	4.56	4.85

the ability of the sparse mask to capture the essential characteristics of face adversarial examples and the strong generalization capability of our method.

Ablation Study and Analysis

To further evaluate our method, we conduct experiments to show the effect of the sparse mask and compare the time cost to baseline methods. We also analyze the functionality of Perturbation Forgery through visualizations. The impact of hyper-parameters is reported in the supplementary materials.

Impact of each mask As argued, the sparse mask is proposed to assist the detector in identifying local adversarial noises present in generative-based adversarial data. As shown in Table 5, the absence of the saliency detection model f_s or the GradCAM model f_c has little effect on the overall system. This is because the regions masked by f_s and f_c are somewhat complementary. However, without the Sobel operation to make the mask sparse, the detector fails entirely in detecting attacks, except for CDA, because the noise in generative-based adversarial data tends to be imbalanced and localized, whereas the noise in CDA is more global. Without the sparsification provided by the Sobel operation, the generated pseudo-noise becomes too dense, preventing the detector from effectively focusing on local noise.

Time Cost of Inference We conducted experiments to calculate the inference time cost for 100 samples on ImageNet100. As shown in Table 6, the time cost of our model is slightly higher than that of LID, LiBRe, and SPAD, and it only takes 0.0485 seconds to process one image. For actual use, a minor increase in time is perfectly acceptable in exchange for a significant increase in detection performance.

Functionality of Perturbation Forgery To validate the functionality of our method, we extract features and flattened noises from adversarial data and Perturbation Forgery and visualize them using 2D t-SNE projection. All adversarial data come from unseen attacks. As shown in Figure 3(a),

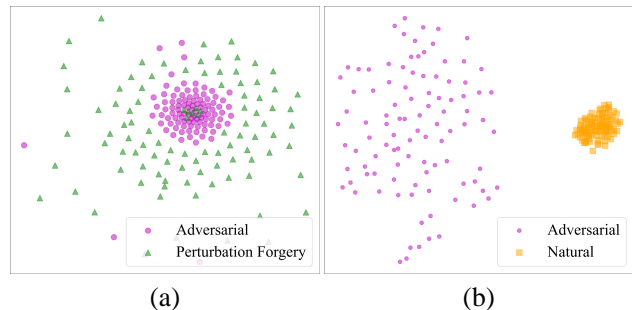


Figure 3: 2D T-SNE visualizations. (a) ImageNet100 flattened noises of adversarial data and Perturbation Forgery. (b) ImageNet100 features extracted by the model trained with Perturbation Forgery.

by continuously perturbing the adversarial noise distribution of a commonly used attack, Perturbation Forgery forms an open covering of noises from unseen attacks. Individual samples float outside of the collective because they are outliers from the noise distribution. As shown in Figure 3(b), by learning to separate natural data from those generated by Perturbation Forgery, the trained detector can effectively distinguish between natural and adversarial data.

Conclusion

In this paper, we explore and define the proximity relationship between adversarial noise distributions by modeling these distributions as multivariate Gaussian. Based on our assumptions and definitions, we establish a perturbation method to craft proximal distributions from a given distribution and demonstrate the existence of an open covering of adversarial noise distributions. After that, we propose the core idea of obtaining a detector with strong generalization abilities against all types of adversarial attacks by learning to distinguish the open covering from the distribution of natural data. Based on this insight, we heuristically propose Perturbation Forgery, which includes noise distribution perturbation, sparse mask generation, and pseudo-adversarial data production, to train an adversarial detector capable of detecting unseen gradient-based, generative-based, and physical adversarial attacks, agnostic to any specific models. The major limitation of our method is that finding the optimal scale parameters for distribution perturbation is challenging. We must rely on continuous experimentation to determine these parameters. However, even if these parameters are not optimal, our method still maintains consistent detection performance across various attacks on multiple general and facial datasets, with a satisfactory inference time cost.

References

- Chen, J.; Chen, H.; Chen, K.; Zhang, Y.; Zou, Z.; and Shi, Z. 2023. Diffusion models for imperceptible and transferable adversarial attack. *arXiv preprint arXiv:2305.08192*.
- Chollet, F. 2017. Xception: Deep Learning with Depthwise Separable Convolutions. In *2017 IEEE Conference on Computer Vision and Pattern Recognition (CVPR)*, 1800–1807.
- Croce, F.; and Hein, M. 2020. Reliable evaluation of adversarial robustness with an ensemble of diverse parameter-free attacks. In *ICML*, 2206–2216. PMLR.
- Deng, J.; Dong, W.; Socher, R.; Li, L.-J.; Li, K.; and Fei-Fei, L. 2009. ImageNet: A large-scale hierarchical image database. In *CVPR*.
- Deng, J.; Guo, J.; Xue, N.; and Zafeiriou, S. 2019. ArcFace: Additive Angular Margin Loss for Deep Face Recognition. In *2019 IEEE/CVF Conference on Computer Vision and Pattern Recognition (CVPR)*, 4685–4694.
- Deng, Z.; Yang, X.; Xu, S.; Su, H.; and Zhu, J. 2021. Libre: A practical bayesian approach to adversarial detection. In *Proceedings of the IEEE/CVF conference on computer vision and pattern recognition*, 972–982.
- Dong, Y.; Liao, F.; Pang, T.; Su, H.; Zhu, J.; Hu, X.; and Li, J. 2018. Boosting Adversarial Attacks with Momentum. In *CVPR*, 9185–9193.
- Du, X.; Wang, Z.; Cai, M.; and Li, Y. 2022. Vos: Learning what you don't know by virtual outlier synthesis. *arXiv preprint arXiv:2202.01197*.
- Duda, R. O.; and Hart, P. E. 1973. *Pattern Classification and Scene Analysis*. New York: John Wiley & Sons.
- Feinman, R.; Curtin, R. R.; Shintre, S.; and Gardner, A. B. 2017. Detecting adversarial samples from artifacts. *arXiv preprint arXiv:1703.00410*.
- Gary, B. H.; Manu, R.; Tamara, B.; and Erik, L.-M. 2007. Labeled faces in the wild: A database for studying face recognition in unconstrained environments. Technical Report 07-49, University of Massachusetts.
- Goodfellow, I. J.; Shlens, J.; and Szegedy, C. 2014. Explaining and Harnessing Adversarial Examples. *arXiv:1412.6572*.
- Gu, Q.; Wang, G.; Chiu, M. T.; Tai, Y.-W.; and Tang, C.-K. 2019. LADN: Local Adversarial Disentangling Network for Facial Makeup and De-Makeup. In *2019 IEEE/CVF International Conference on Computer Vision (ICCV)*, 10480–10489.
- He, K.; Zhang, X.; Ren, S.; and Sun, J. 2016. Deep residual learning for image recognition. In *CVPR*, 770–778.
- He, Y.; Yu, N.; Keuper, M.; and Fritz, M. 2021. Beyond the Spectrum: Detecting Deepfakes via Re-Synthesis. In *Proceedings of the Thirtieth International Joint Conference on Artificial Intelligence, IJCAI-21*, 2534–2541. International Joint Conferences on Artificial Intelligence Organization. Main Track.
- Hu, S.; Liu, X.; Zhang, Y.; Li, M.; Zhang, L. Y.; Jin, H.; and Wu, L. 2022. Protecting Facial Privacy: Generating Adversarial Identity Masks via Style-Robust Makeup Transfer. In *Proceedings of the IEEE/CVF Conference on Computer Vision and Pattern Recognition (CVPR)*, 15014–15023.
- Karras, T.; Aila, T.; Laine, S.; and Lehtinen, J. 2017. Progressive growing of gans for improved quality, stability, and variation. *arXiv preprint arXiv:1710.10196*.
- Kim, H. 2020. Torchattacks: A pytorch repository for adversarial attacks. *arXiv preprint arXiv:2010.01950*.
- Krizhevsky, A.; Hinton, G.; et al. 2009. Learning multiple layers of features from tiny images. *Technical report*.
- Kurakin, A.; Goodfellow, I.; and Bengio, S. 2016. Adversarial Machine Learning at Scale. *arXiv:1611.01236*.
- Liang, S.; Li, Y.; and Srikant, R. 2017. Enhancing the reliability of out-of-distribution image detection in neural networks. *arXiv preprint arXiv:1706.02690*.
- Lin, J.; Song, C.; He, K.; Wang, L.; and Hopcroft, J. E. 2019. Nesterov Accelerated Gradient and Scale Invariance for Adversarial Attacks. In *ICLR*.
- Luo, Y.; Zhang, Y.; Yan, J.; and Liu, W. 2021. Generalizing Face Forgery Detection with High-frequency Features. In *2021 IEEE/CVF Conference on Computer Vision and Pattern Recognition (CVPR)*, 16312–16321.
- Ma, X.; Li, B.; Wang, Y.; Erfani, S. M.; Wijewickrema, S.; Schoenebeck, G.; Song, D.; Houle, M. E.; and Bailey, J. 2018. Characterizing Adversarial Subspaces Using Local Intrinsic Dimensionality. *arXiv:1801.02613*.
- Madry, A.; Makelov, A.; Schmidt, L.; Tsipras, D.; and Vladu, A. 2017. Towards Deep Learning Models Resistant to Adversarial Attacks. *arXiv:1706.06083*.
- Naseer, M.; Khan, S.; Hayat, M.; Khan, F. S.; and Porikli, F. 2021. On generating transferable targeted perturbations. In *Proceedings of the IEEE/CVF International Conference on Computer Vision*, 7708–7717.
- Naseer, M. M.; Khan, S. H.; Khan, M. H.; Shahbaz Khan, F.; and Porikli, F. 2019. Cross-domain transferability of adversarial perturbations. *Advances in Neural Information Processing Systems*, 32.
- Ojha, U.; Li, Y.; and Lee, Y. J. 2023. Towards universal fake image detectors that generalize across generative models. In *Proceedings of the IEEE/CVF Conference on Computer Vision and Pattern Recognition*, 24480–24489.
- Qin, X.; Zhang, Z.; Huang, C.; Gao, C.; Dehghan, M.; and Jagersand, M. 2019. BASNet: Boundary-Aware Salient Object Detection. In *The IEEE Conference on Computer Vision and Pattern Recognition (CVPR)*.
- Selvaraju, R. R.; Cogswell, M.; Das, A.; Vedantam, R.; Parikh, D.; and Batra, D. 2017. Grad-cam: Visual explanations from deep networks via gradient-based localization. In *Proceedings of the IEEE international conference on computer vision*, 618–626.
- Sharif, M.; Bhagavatula, S.; Bauer, L.; and Reiter, M. K. 2016. Accessorize to a crime: Real and stealthy attacks on state-of-the-art face recognition. In *Proceedings of the 2016 acm sigsac conference on computer and communications security*, 1528–1540.

- Shi, Y.; Ling, H.; Wu, L.; Shen, J.; and Li, P. 2020. Learning refined attribute-aligned network with attribute selection for person re-identification. *Neurocomputing*, 402: 124–133.
- Tan, C.; Zhao, Y.; Wei, S.; Gu, G.; and Wei, Y. 2023. Learning on gradients: Generalized artifacts representation for gan-generated images detection. In *Proceedings of the IEEE/CVF Conference on Computer Vision and Pattern Recognition*, 12105–12114.
- Tong, L.; Chen, Z.; Ni, J.; Cheng, W.; Song, D.; Chen, H.; and Vorobeychik, Y. 2021. Facesec: A fine-grained robustness evaluation framework for face recognition systems. In *Proceedings of the IEEE/CVF Conference on Computer Vision and Pattern Recognition*, 13254–13263.
- Tramèr, F.; Kurakin, A.; Papernot, N.; Goodfellow, I.; Boneh, D.; and McDaniel, P. 2018. Ensemble Adversarial Training: Attacks and Defenses. In *International Conference on Learning Representations*.
- Wang, Q.; Xian, Y.; Ling, H.; Zhang, J.; Lin, X.; Li, P.; Chen, J.; and Yu, N. 2023a. Detecting Adversarial Faces Using Only Real Face Self-Perturbations. In *IJCAI*, 1488–1496. Main Track.
- Wang, S.-Y.; Wang, O.; Zhang, R.; Owens, A.; and Efros, A. A. 2020. CNN-generated images are surprisingly easy to spot... for now. In *Proceedings of the IEEE/CVF conference on computer vision and pattern recognition*, 8695–8704.
- Wang, X.; and He, K. 2021. Enhancing the transferability of adversarial attacks through variance tuning. In *CVPR*, 1924–1933.
- Wang, Z.; Bao, J.; Zhou, W.; Wang, W.; Hu, H.; Chen, H.; and Li, H. 2023b. Dire for diffusion-generated image detection. In *Proceedings of the IEEE/CVF International Conference on Computer Vision*, 22445–22455.
- Wu, W.; Su, Y.; Lyu, M. R.; and King, I. 2021. Improving the Transferability of Adversarial Samples with Adversarial Transformations. In *CVPR*, 9020–9029.
- Xue, H.; Araujo, A.; Hu, B.; and Chen, Y. 2024. Diffusion-based adversarial sample generation for improved stealthiness and controllability. *Advances in Neural Information Processing Systems*, 36.
- Yang, X.; Dong, Y.; Pang, T.; Su, H.; Zhu, J.; Chen, Y.; and Xue, H. 2021. Towards Face Encryption by Generating Adversarial Identity Masks. In *ICCV*, 3877–3887.
- Yin, B.; Wang, W.; Yao, T.; Guo, J.; Kong, Z.; Ding, S.; Li, J.; and Liu, C. 2021. Adv-Makeup: A New Imperceptible and Transferable Attack on Face Recognition. In *Proceedings of the Thirtieth International Joint Conference on Artificial Intelligence, IJCAI-21*, 1252–1258. International Joint Conferences on Artificial Intelligence Organization.
- Yoon, J.; Hwang, S. J.; and Lee, J. 2021. Adversarial purification with score-based generative models. In *ICML*, 12062–12072.
- Zhang, H.; Yu, Y.; Jiao, J.; Xing, E.; El Ghaoui, L.; and Jordan, M. 2019. Theoretically principled trade-off between robustness and accuracy. In *ICML*, 7472–7482.
- Zhang, S.; Liu, F.; Yang, J.; Yang, Y.; Li, C.; Han, B.; and Tan, M. 2023. Detecting adversarial data by probing multiple perturbations using expected perturbation score. In *International Conference on Machine Learning*, 41429–41451. PMLR.
- Zhang, Z.; and Sabuncu, M. 2018. Generalized Cross Entropy Loss for Training Deep Neural Networks with Noisy Labels. In Bengio, S.; Wallach, H.; Larochelle, H.; Grauman, K.; Cesa-Bianchi, N.; and Garnett, R., eds., *NeurIPS*, volume 31.
- Zhao, A.; Chu, T.; Liu, Y.; Li, W.; Li, J.; and Duan, L. 2023. Minimizing maximum model discrepancy for transferable black-box targeted attacks. In *Proceedings of the IEEE/CVF Conference on Computer Vision and Pattern Recognition*, 8153–8162.

Detecting Adversarial Data via Perturbation Forgery

Appendix

Proofs

Theorem Proofs

Proof of Theorem 1.

Proof. Denoting the distribution of natural sample \mathbf{x} as P , we use the 1-Wasserstein distance as the metric $d(\cdot, \cdot)$, to prove the theorem.

1) We denote the independent adv-noise distribution of η_i as $Q_i \in \mathcal{P}_a$ where $\eta_i = \hat{\mathbf{x}}_i - \mathbf{x}$, and a zero-distribution as P where its mean and variance are zero vectors. Then the 1-Wasserstein distance between η_i and η_j can be bound by its metric property and dual form:

$$\begin{aligned} W_1(Q_i, Q_j) &\leq W_1(Q_i, P) + W_1(Q_j, P) \\ &\leq \sup_{\|g\|_L \leq 1} \mathbb{E}_{\eta_i \sim Q_i}[g(\eta_i)] - \mathbb{E}_{\mathbf{x} \sim P}[g(\mathbf{x})] \\ &\quad + \sup_{\|g\|_L \leq 1} \mathbb{E}_{\eta_j \sim Q_j}[g(\eta_j)] - \mathbb{E}_{\mathbf{x} \sim P}[g(\mathbf{x})] \\ &\leq 2\epsilon, \end{aligned}$$

where $\|g\|_L$ is the Lipschitz constant of function g w.r.t. the norm induced by the metric here.

2) Consider two random noise $\eta_i \sim \mathcal{N}_i(\mu_i, \sigma_i^2 \mathbf{I}_d)$ and $\eta_j \sim \mathcal{N}_j(\mu_j, \sigma_j^2 \mathbf{I}_d)$. While it's mean and variance satisfied that $\|\mu_i - \mu_j\| \leq \epsilon$ and $|\sigma_i - \sigma_j| \leq \epsilon$. then the 2-Wasserstein distance between η_1 and η_2 is

$$\begin{aligned} W_2(\eta_i, \eta_j)^2 &= \|\mu_i - \mu_j\|^2 + \text{trace}(\sigma_i^2 \mathbf{I}_d + \sigma_j^2 \mathbf{I}_d \\ &\quad - 2 \left((\sigma_j^2 \mathbf{I}_d)^{1/2} \sigma_i^2 \mathbf{I}_d (\sigma_j^2 \mathbf{I}_d)^{1/2} \right)^{1/2}) \\ &\leq \epsilon_\mu^2 + d \cdot \epsilon_\sigma^2, \end{aligned}$$

where $(\sigma_i^2 \mathbf{I}_d)^{1/2}$ denotes the principal square root of $\sigma_i^2 \mathbf{I}_d$. \square

Corollary 1. 1) All noise distributions proximal to the known adversarial distribution $p(\boldsymbol{\eta})$ form an open ϵ -ball centered on $p(\boldsymbol{\eta})$, denoting as $\mathcal{P}_\epsilon = \{p(\boldsymbol{\eta}_i) | d(p(\boldsymbol{\eta}_i), p(\boldsymbol{\eta})) < \epsilon\}$, and also form a metric space $(\mathcal{P}_\epsilon, d)$.

2) The adv-noise distribution set is also located in this ball: $\mathcal{P}_a \subset \mathcal{P}_\epsilon$.

3) Based on the properties of the complete metric space $(\mathcal{P}_\epsilon, d)$, for all subset $\mathcal{P}_i \subset \mathcal{P}_\epsilon$, there exists a finite open covering of the subset: $\mathcal{P}_i \subset \{G_c\}_{c \in J}$.

Proof. 1) Consider 1-Wasserstein distance as metric d , for $\forall Q_i, Q_j \in \mathcal{P}_\epsilon$, we have

$$W_1(Q_i) \geq 0. \quad W_1(Q_i, Q_j) = 0 \text{ if and only if } Q_i = Q_j. \quad (13)$$

$$W_1(Q_i, Q_j) = W_1(Q_j, Q_i). \quad (14)$$

$$W_1(Q_i, Q_j) \leq W_1(Q_i, P) + W_1(Q_j, P). \quad (15)$$

Therefore, $(\mathcal{P}_\epsilon, d)$ is a metric space.

2) It is obvious according to the definition of \mathcal{P}_ϵ .

3) For any subset $\mathcal{P}_i = \{p_{i1}, p_{i2}, \dots, p_{in}\} \subset \mathcal{P}_\epsilon$, we can construct several spherical subsets $\{\mathcal{P}_{ij}\}$ with p_{i1} as the center and $|\epsilon - d(p_{i1}, p(\boldsymbol{\eta}))|$ as the radius. $\{\mathcal{P}_{ij}\}$ is a open covering of \mathcal{P}_i . \square

Experimental Details

Dataset

CIFAR10 CIFAR10 consists of a training set of 50,000 images and a test set of 10,000 images, each with a resolution of 32x32 pixels. These images are divided into 10 different classes. The classes represent everyday objects such as airplanes, automobiles, birds, cats, deer, dogs, frogs, horses, ships, and trucks.

ImageNet100 ImageNet-100 is a subset of ImageNet (Deng et al. 2009), comprising 100 classes selected from the original ImageNet dataset, each containing a substantial number of high-resolution images, with 1,300 images per class.

Makeup Makeup comprises images of faces with and without makeup. These images are collected from various sources to ensure a diverse representation of facial features, makeup styles, and skin tones. There are 333 before-makeup images and 302 after-makeup images.

CelebA-HQ CelebA-HQ dataset is a high-quality version of the original CelebA dataset. CelebA-HQ consists of 30,000 high-resolution images of celebrity faces, derived from the CelebA dataset through a progressive GAN-based upsampling and quality enhancement process. Each image in CelebA-HQ is 1024x1024 pixels.

LFW LFW contains 13,233 labeled images of 5,749 different individuals collected from the internet, each image is labeled with the name of the person pictured. LFW images vary widely in terms of lighting, facial expression, pose, and background, closely reflecting real-world conditions. The images are provided in a resolution of 250x250 pixels, and the faces are roughly aligned based on the eye coordinates.

Adversarial Attacks

Gradient-based attacks We use Torchattacks (Kim 2020) to implement adversarial attacks. The victim models used for adversarial data generation are ResNet-50 (He et al. 2016) for ImageNet, WideResNet-28 for CIFAR10 (Krizhevsky, Hinton et al. 2009), and ArcFace (Deng et al. 2019) for face attacks.

Generative-model-based attacks For CDA, we use the pre-trained generator which has been trained on ImageNet with a relativistic loss against ResNet152. For TTP, we use the pre-trained-generators trained against ResNet50 for 8 target labels, they are: Grey Owl(24),Goose(99),French

Table 7: Detection AUC(%) against various gradient-based attacks on CIFAR-10 ($\epsilon = 4/255$).

Detector	BIM	PGD	RFGSM	DIM	MIM	NIM	VNIM	SNIM	AA
SPAD (Wang et al. 2023a)	99.51	99.38	99.35	99.52	99.66	99.85	99.47	99.63	99.74
EPSAD (Zhang et al. 2023)	99.99	99.98	99.98	99.99	99.99	99.99	99.99	99.99	99.99
ours	99.65	99.65	99.68	99.47	99.80	99.80	99.76	99.64	99.88

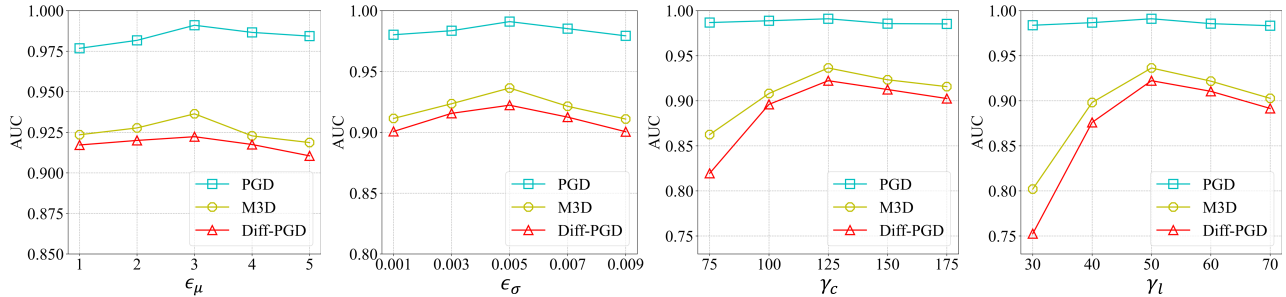


Figure 4: The influence of parameters on the detection performance.

Bulldog(245), Hippopotamus(344), Cannon(471), Fire Engine(555), Parachute(701), Snowmobile(802). We generate 1000 adversarial examples for each label and randomly select 125 adversarial examples for each label. For M3D, its settings are consistent with TTP. For Diff-PGD, we use the global attack to craft adversarial examples, target classifier is ResNet50, the diffusion model accelerator is ddim50, the reverse step in SDEdit is 3, and the iteration number of PGD is 10, the step size is 2. For Diff-attack, the target classifier is ResNet50, DDIM sample steps are set as 20, and iterations to optimize the adversarial image are set as 30. For the methods mentioned above, we all use the authors’ implementation to craft adversarial examples.

Face attacks For face attacks, 1 gradient-based attack TIPIM (Yang et al. 2021), two GAN-based attacks including AdvMakeup (Yin et al. 2021) and AMT-GAN (Hu et al. 2022), and 3 physical attacks including Adv-Sticker (Tong et al. 2021), Adv-Glasses (Sharif et al. 2016), and Adv-Mask (Tong et al. 2021) produce face adversarial samples by attacking the victim face model ArcFace (Deng et al. 2019).

Baselines

Adversarial detection For LiBRE¹, we trained a ResNet-50 on ImageNet100 and finetuned it using the authors’ implementation, the parameters were kept consistent with theirs. For EPSAD², we use the pre-trained models provided by the authors and follow the instructions by the authors to get the detection results. Due to the time-consuming nature of computing EPS, we evaluated 1,000 images for each attack method on ImageNet-100.

Synthetic image detection Since existing adversarial example detection methods do not address adversarial examples based on generative models, we compared our method with various synthetic image detection methods to effectively validate its effectiveness. We conducted detection experiments on adversarial examples

based on generative models using the following methods: CNN-Detection(Wang et al. 2020)³, LGrad(Tan et al. 2023)⁴, Universal-Detector(Ojha, Li, and Lee 2023)⁵, and DIRE(Wang et al. 2023b)⁶. We conducted experiments using the pre-trained models and authors’ implementation code of the above methods.

Implementation Details

Experiments are implemented using 2 Nvidia DeForce RTX 3090 GPUs. For training detectors, we use an Adam optimizer with a learning rate of $2e-4$, momentum of 0.9, and weight decay of $5e-6$.

Data pre-processing We resize images to 32×32 for CIFAR10, 256×256 for ImageNet100, Makeup and CelebA-HQ, and 112×112 for LFW. For ImageNet100, after resizing, we center-crop the images to 224×224 . After that, all of the images are resized to 256×256 followed by random horizontal flip and normalization.

Noise distribution As related in the main paper, we flatten the generated noise to a vector and estimate its distribution. However, for a noise with a shape of $256 \times 256 \times 3$, the length of the corresponding flattened noise is 196,608, making it impossible to run the algorithm on a single GPU. Therefore, we fix the size of noise to $32 \times 32 \times 3$, and concatenate several sampled pseudo noises to fit the larger image.

Experiment on CIFAR-10

We conduct experiments to detect gradient-based attacks on CIFAR10. As reported in Table 7, our method demonstrates effective detection (achieving an AUC score over 0.99) across a variety of attack methods, validating our assumptions of the noise distribution proximity.

¹<https://github.com/thudzj/ScalableBDL/tree/efficient/exps>

²<https://github.com/ZSHsh98/EPS-AD>

³<https://github.com/peterwang512/CNNDetection>

⁴<https://github.com/peterwang512/CNNDetection>

⁵<https://github.com/Yuheng-Li/UniversalFakeDetect?tab=readme-ov-file#weights>

⁶<https://github.com/ZhendongWang6/DIRE>

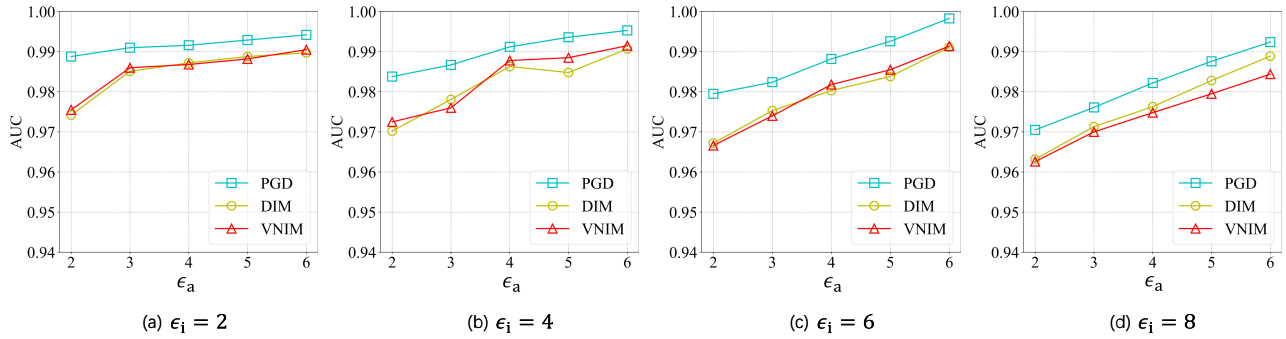


Figure 5: The influence of attack intensity on the detection performance.



Figure 6: Natural images and corresponding pseudo-adversarial images generated by Perturbation Forgery.

Impact of Parameters We select typical attacks and present curves in Figure 4 to depict the impact of parameters on the detection performance. The parameters ϵ_μ and ϵ_σ have little effect on detecting PGD, while γ_c and γ_l have significant effects on detecting M3D and Diff-PGD. This might be because, regardless of whether ϵ_μ and ϵ_σ are large or small, the accuracy of forming the open coverage remains unaffected as long as the data is sufficient. However, too small thresholds lead to adding pseudo-noise to insensitive and low-frequency regions, while too large thresholds result in extremely sparse pseudo-noise that is far from the adversarial noise distribution.

To explore the impact of perturbation intensity of attacks, we select typical attacks and present the curves in Figure 5, where ϵ_a denotes the intensity of unseen attacks and ϵ_i denotes the intensity of the initial attack for Perturbation Forgery. We can see that the detector trained with a minor ϵ_i is able to detect adversarial data generated with a larger ϵ_a . When ϵ_i is larger, adversarial data generated with a minor ϵ_a is not easy to detect. This might be because adversarial noises generated with a higher ϵ_a tend to be more obvious to detect. When ϵ_a is too small than ϵ_i , the distance between the initial attack noise and the unseen attack noise is too far away, reducing the detection performance.

Limitations

The major limitation of our method is that finding the optimal scale parameters for distribution perturbation is challenging. We must rely on continuous experimentation to determine these parameters. Specifically, we initiate param-

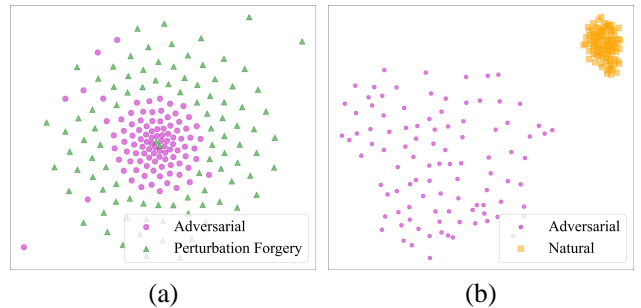


Figure 7: 2D T-SNE visualizations. (a) CIFAR-10 flattened noises of adversarial data and Perturbation Forgery. (b) CIFAR-10 features extracted by the model trained with Perturbation Forgery.

eters of uniform distribution as $\epsilon_\mu = 1$ and $\epsilon_\sigma = 0.001$, and adjust them using a small step factor. Finally, we find the experiment results when $\epsilon_\mu = 3$ and $\epsilon_\sigma = 0.005$ are close to optimal. However, even if these parameters are not optimal, our method still maintains consistent detection performance across various attacks on multiple general and facial datasets, with a satisfactory inference time cost.

More Visualization Results

Visualization on CIFAR-10

We extract features and flattened noises from adversarial data and Perturbation Forgery from CIFAR-10 and visualize them using 2D t-SNE projection in Figure 7.

Visualization Examples

Some examples of Perturbation Forgery at $\epsilon = 4/255$ are shown in Figure 6.